

**SCALING RELATIONSHIPS FOR THERMALLY DRIVEN  
REDISTRIBUTION OF MOISTURE THROUGH PARTIALLY  
SATURATED POROUS MEDIA**

**by**

**F.T. Dodge**

**R.T. Green**

## ABSTRACT

Scaling laws are developed using similarity theory to identify relationships among heat and mass transfer mechanisms at the laboratory ( $10^{-1}$  to  $10^0$  m), field ( $10^1$  m) and mountain ( $10^2$  and  $10^3$  m) scales. The scaling laws are formulated for use in predicting the rates of thermally driven dry out and rewetting in geologic media by relating information gained at smaller scales, where experimentation can be performed, to larger scales, hopefully providing insight into the performance of a geologic high-level waste (HLW) repository. Because the driving mechanisms are different for the heating and cooling periods of a HLW repository, separate sets of scaling laws are developed for each period. These scaling laws are developed from a set of simplified conceptual models derived specifically for the buildup of gas pressure and attendant drying out of the medium during the initial period of large heating rates and for the rewetting of the dried out region during the later cooling phase. The conceptual models are based on the general theory of two-component, two-phase flow in heated, partially saturated porous media. The models are characterized in terms of dimensionless parameters. For example, a gas Advection Number,  $Ad_g$ , identifies the importance of gas pressure gradients relative to buoyancy-induced body forces during the heating period. Similarly, a liquid Advection Number,  $Ad_l$ , identifies the importance of liquid pressure gradients relative to buoyancy-induced body forces during the cooling period. The dimensionless parameters are useful in the identification of different classes of flow regimes formed as a function of a specified heat load. The pressure, velocity, and time scaling laws developed from the conceptual models can be used to interpret or scale-up the responses measured in laboratory- and field-scale experiments in terms of repository responses, and to guide numerical simulations of these responses.

## INTRODUCTION

Yucca Mountain (YM) in southwest Nevada has been proposed as the site for a high-level radioactive waste (HLW) repository. This site has a semi-arid climate, and the underground repository itself is to be located in the unsaturated zone of the host rock; both of these attributes are expected to contribute to long-term waste isolation. These two favorable conditions do create, however, many challenges in evaluating the predicted performance of the repository. In addition, it is widely recognized that the decay heat produced by HLW will likely have a significant impact on both the pre- and post-closure performance of the YM repository. The task of delineating which aspects of that impact are favorable to waste isolation and which are adverse is a difficult technical undertaking because of the hydrothermal regimes involved, the heterogeneity of the geologic media, and the variety of time and space scales.

Recent numerical modeling studies (Buscheck and Nitao, 1993; Lichtner and Walton, 1994) suggest that the thermal evolution of a geologic HLW repository can be divided into three distinct periods: (i) heating, (ii) transitional, and (iii) cooling. During the heating period, radioactive decay of the waste causes a monotonic rise in temperature of the host rock that may last hundreds of years. The heating vaporizes much of the liquid water in the partially saturated rock pores near the waste packages. Water, in the form of vapor, is consequently driven away from the waste packages by gas-phase pressure gradients caused by the heating, with the result that the rock dries out. Later, after the rate of radioactive decay has decreased to a low level, the temperatures near the waste packages decrease. Water transport in the rock is then predominantly in the liquid phase, and this liquid water tends to return to the vicinity of the waste packages as a result of capillary pressure gradients. This is the cooling period. A transitional period occurs between the heating and cooling periods during which water is transported as both vapor and liquid (referred to here as moisture), potentially in opposing directions. Starting from this thermal evolution model, studies by Ramspott (1991); Nitao et al. (1992); Buscheck and Nitao (1992, 1993, 1994); Wilder

(1993); and Andrews et al. (1994) suggest that proper selection of the thermal loading could potentially extend the time period that the waste packages remain dry. Preliminary findings from such studies have led to an "extended-dry" repository thermal regime that could: (i) extend the period of radionuclide containment in the engineered barrier system (EBS), and (ii) reduce the sensitivity of total-system performance to hydrologic variability. The potential benefits of an elevated heat load strategy, however, are not universally held. Pruess and Tsang (1993, 1994) note that increasing the thermal load might not necessarily decrease the exposure of the waste canisters to moisture.

The present study focused on the coupled thermal/hydrologic interactions that determine the effect of heat sources on the redistribution of moisture in partially saturated media. Scaling laws were developed to identify similarities among the heat and mass transfer mechanisms for the heating and cooling periods at the laboratory ( $10^{-1}$  to  $10^0$  m), field ( $10^1$  m) and mountain ( $10^2$  to  $10^3$  m) scales. If valid, the scaling laws can provide a means of relating thermally driven moisture redistribution through porous media observed at smaller scales to predictions of heat and mass transfer at larger scales (i.e., laboratory to field scale or field to mountain scale). Dimensionless groups developed with the scaling laws can be used to identify different classes of liquid and vapor flow regimes that could result from different thermal loading strategies.

## CONCEPTUAL MODELS AND SIMILARITY

### ANALYSIS OF THERMOHYDROLOGIC PERIODS

The general theory of two-phase, multi-component flows in partially saturated porous, fractured media is still under active development (Narasimhan, 1982; Wang and Narasimhan, 1986; Rasmussen and Evans, 1989). These flows are inherently three-dimensional (3D), which complicates both their analysis and experimentation. Further, many types of phenomena can occur, such as a countercurrent flow of liquid and vapor much like a heat pipe (Pruess, 1985; Lichtner and Walton, 1994); the phases can also be partially or completely segregated, for example, liquid transport may be confined to the lower permeability parts of the medium (e.g., the matrix) while gas transport occurs primarily in the higher permeability parts (e.g., fractures). The physics of the flows in some cases are dominated by mechanisms (e.g., gas pressure gradients) that are negligible in other cases. For all these reasons, it is difficult to extract from the general theory guidance on the design and evaluation of experiments and numerical simulations. Simplified, conceptual models are needed for these purposes and to aid in evaluating the relative importance of various physical mechanisms for specific applications. The models can also be used to develop "scaling laws" for interpreting experiments conducted, for example, in a laboratory in terms of the results that should be anticipated in a field-scale experiment.

In this section, such conceptual models are developed by simplifying and specializing the general theory. Scaling laws are developed from these models by casting the equations of the models in dimensionless form. This process is usually called a "similitude" analysis (Bear, 1972; Baker et al., 1973; Miller, 1980) to distinguish it from a "dimensional" analysis in which the variables and parameters that are thought to influence a flow are grouped together to form dimensionless terms by dimensional considerations alone (Fox and McDonald, 1978; Corey, 1986). Both methods yield a "similarity analysis" but the similitude

method provides much more physical insight, although it also requires more knowledge since the governing equations must be developed first.

## GENERAL APPLICATION OF SIMILARITY ANALYSIS

A scale model of a larger system will simulate the response of a larger system if the scale model is geometrically, kinematically, dynamically, and constitutively similar to the large system. The definitions of these types of similarity are (Baker et al., 1973):

- (i) Geometric Similarity—The model has the same shape and proportions as the large system for those parts of the system in which geometry affects the responses
- (ii) Kinematic Similarity—The velocity at each point in the model has the same direction as that in the large system, and the magnitude of the model velocities is a constant multiple of the larger system velocities
- (iii) Dynamic Similarity—The forces, and accelerations at each point in the model have the same direction as those in the large system, and their magnitudes are a constant multiple of those in the large system
- (iv) Constitutive Similarity—The constitutive properties of the model materials (e.g., the relation between relative permeability and saturation) have the same functional relationship as the large system materials

When the conditions for all four similarities are fulfilled, the response of the model is identical to that of the large system, at homologous locations and homologous times.

When a scale model is designed so that all of its relevant dimensionless groups have identical numerical values as those of the larger system it is meant to simulate, the model satisfies all four kinds

of similarity, and the dimensionless groups can be used to define unambiguous “scaling factors” (ratios of similar effects or phenomena in the model and the larger system) to interpret or “scale up” the model responses to full scale values. More commonly, it is found, however, that not all the dimensionless groups of the scale model can be made to have the same value as those of the larger system; for example, because of the difference in geometric scales, a particular dimensionless group may require that the surface tension or the viscosity of the model fluid be larger (or smaller) than that of any known liquid. In that case, the scale model will not satisfy all four kinds of similarity, and the model responses are “distorted” in some (possibly unknown) way compared to the larger system. Even so, it may still be possible to use the model to investigate accurately some limited part of the larger system response. However, in that case, conceptual and mathematical models are needed to help “scale up” the scale model responses.

Because of the widely varying spatial scales of the proposed repository (very small matrix pores, a system of somewhat larger fractures, and a very large affected zone) and the long time duration over which the responses occur, the scale models utilized in the present study (Green, et al, 1995) are distorted in the sense described above. In particular, it was not feasible to construct laboratory models with a sufficiently small geometric scale (approximately 1 to 1000) that would realistically represent the interaction between the matrix and the system of fractures. Thus, fractures are not considered explicitly in the scaling law analyses; it might be noted that a similar difficulty also occurs in numerical models. Further, in the laboratory scale models, it was not possible to represent all the relevant physical effects of interest in the same relative proportions; for example, capillary pressures in the model matrix were nearly equal in magnitude to those in the larger system, but gas-phase pressures were sometimes smaller than full scale, depending on the particular test.

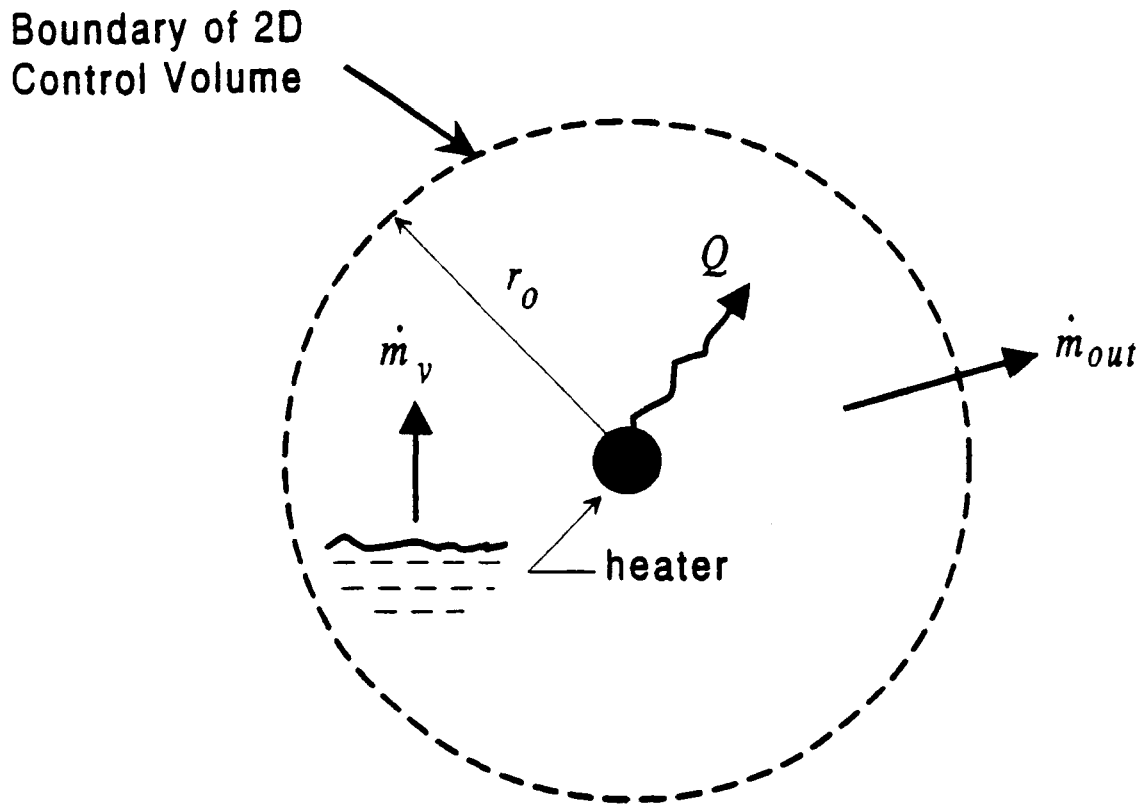


Figure 1. Sketch of control volume used for the conceptual model of pressure-driven gas flow during the heating phase

To help overcome these unavoidable distortions in the scale model, idealized mathematical models for several important responses were developed to aid in designing the scale models and the tests and in interpreting the test results. These conceptual models covered the three different response periods discussed earlier.

- **Heating period.** - A conceptual model was developed to predict the most important factors that establish heating conditions for which large gas-phase pressure gradients and velocities will be created, and the time duration over which such responses can be sustained, with the aim of investigating the potential drying-out of the volume around the heaters.

- **Cooling period.** - A conceptual model was developed to predict the most important factors that establish the (i) re-wetting rate of a dried out region after the heating rate is reduced, and (ii) the time duration required for substantially complete re-wetting.
- **Transition period.** - No special model was developed for this period since the cooling period model was sufficiently general to include the transition between the heating and cooling periods; the transition period was not, however, investigated explicitly in the model tests.

As shown in the discussion below, an important result of the conceptual models is the definition of a new dimensionless group, named the gas or liquid Advection number (for the heating or cooling periods, respectively). When the model value of the Advection number is of the same magnitude as the Advection number of the larger system, the gross features of the gas-phase or liquid-phase flow induced by heating should be the same for both the model and the larger system (assuming that the initial and boundary conditions of the model adequately represent the larger system). Although other aspects of the model responses may be distorted, the similarity of the gross features allows the model test measurements of drying out and rewetting to be scaled up reliably to predict the analogous responses of the larger system.

## CONCEPTUAL MODEL FOR THE HEATING PERIOD

During the heating period, the rate at which heat is released has a dominant influence on thermohydrologic responses. Large heating rates can lead to a so-called hot or extended-dry repository, while smaller heating rates lead to a cool or moist repository. The DOE G-Tunnel heater tests (Zimmerman et al., 1986; Ramirez, 1991) and numerical simulations and laboratory tests (Green et al., 1995) indicate that one of the distinguishing features of the heating regime is whether large pressure gradients develop in the gas phase. If they do, the repository tends to dry out because the large gas flow produced by the pressure gradients transports significant amounts of water, in the form of vapor, away

from the heated region. Since the source of this water is the liquid water initially in the porous matrix, the repository tends to dry out. Consequently, the focus of the conceptual model developed for the heating regime is the occurrence of significant gas-phase pressure gradients.

The conceptual model for the heating phase is a generalization of the similar case in which buoyancy is the only important force driving the flow. For this kind of buoyancy-driven flow pattern, Darcy's law for the gas flow can be expressed in the following dimensionless form (Green et al., 1993):

$$\hat{V}_g = -\hat{\nabla}\hat{p}_g + \theta\hat{e}_z \quad (1)$$

(A list of notation, with units, is given at the end of the paper). The caret (^) indicates a dimensionless quantity;  $V_g$  is gas velocity,  $p_g$  is gas pressure  $\theta = \Delta T/\Delta T_0$  is the dimensionless temperature change of the fluid; and  $\Delta T_0$  is a "characteristic" temperature increase of the heated region. The nonhydrostatic gas pressure has been made dimensionless by normalizing the pressure with respect to a "characteristic" nonhydrostatic pressure magnitude:

$$\hat{p}_{go} = \hat{p}_g \left[ \rho_{go} g L \beta_g \Delta T_0 \right] \quad (2)$$

in which  $\rho_{go}$  is the characteristic, or representative, gas density of the flow,  $\beta$  is the thermal coefficient of gas, and  $L$  is the characteristic length scale of the flow, and the Z-axis of the coordinate system is vertically upward. The "characteristic" parameters used in Eqs. (1) and (2) are meant to represent the physical problem of interest; for that reason, they must be chosen or computed from the conditions imposed on the problem.

Similarly, the gas flow velocity can be made dimensionless using a characteristic velocity  $V_{go}$  of the flow:

$$V_{go} = \left[ \frac{k k_{rel,g}}{\mu_g} (\rho_{go} g \beta_g \Delta T_o) \right] \quad (3)$$

where  $k$  is the permeability,  $k_{rel,g}$  is the relative permeability of the medium for gas flow, and  $\mu_g$  is the gas viscosity. The gas phase has been assumed to be "continuous;" that is, all the gas is connected and pressure gradients are transmitted to the entire gas volume. The dimensionless variables in Eq. (1) have a numerical range from zero to about one, that is, they are of order unity. The magnitudes of the characteristic nonhydrostatic pressure and velocity, Eqs. (2) and (3), depend on the heating through the characteristic temperature increase  $\Delta T_o$ . Because of the small numerical value of  $\beta_g$ , the characteristic nonhydrostatic pressure is much smaller than the characteristic hydrostatic pressure,  $\rho_{go} g L$ , and the buoyancy-induced circulation has a relatively small characteristic velocity.

Pressure and velocity scale factors, which are needed to interpret or scale-up measurements made on a scale model to a larger system, can be derived from Eqs. (2) and (3). For example, the pressure scale factor for this buoyancy-driven flow is derived by forming the ratio of the characteristic pressure definitions for both the model system and the larger system:

$$\text{Pressure scale factor} = \frac{(\rho_{go} g L \beta_g \Delta T_o)_{\text{model system}}}{(\rho_{go} g L \beta_g \Delta T_o)_{\text{larger system}}} \quad (4)$$

Pressure measurements obtained experimentally from the model system can be divided by this "pressure scale factor" to predict the pressure responses of the larger system. The velocity scale factor can

be determined in the same way from Eq. (3). The time scale factor is likewise computed as the ratio of the factor "length scale/velocity scale" for the two systems.

For a flow driven predominantly by buoyancy, the velocity scale is determined, as shown by Eq. (3) by the interaction of two *generalized* forces, namely buoyancy and viscous forces. Thus, only one characteristic velocity can be defined, and the time scale factor is unambiguous. For other flows, there may be more than two generalized forces (for example, there may also be a nonbuoyancy pressure gradient), and so more than one characteristic velocity can be defined formally. All the characteristic velocities must be equal, though, and this requirement generally will place restrictions on the physical scale model; for example, the temperature increase may no longer be allowed to be chosen arbitrarily in the model but must be related to the value of some other parameter such as the nonbuoyancy pressure gradient in order to make the various characteristic velocities equal.

To determine when large pressure gradients occur in a heated porous medium, characteristic pressure, velocity, and time scales of a more general form than Eqs. (2) and (3) are needed. These more general relations are derived from the conceptual models described below.

### **Control Volume Analysis of a Heated Partially Saturated Region**

An imaginary control volume encompassing the region of high gas pressures, as shown in Figure 1, is used to develop the conceptual model for the heating period. A 2D geometry (i.e., a line heat source) is considered but the same analysis would hold for area heaters and 3D geometries, except for some

numerical factors of order unity. The spatial extent of the control volume is specified by a characteristic length,  $L$ , that can be the same as the control volume radius  $r_o$ .

**Gas Flow at the Control Volume Boundary.** Considering first only the advective component of the gas flow out of the control volume,  $\dot{m}_{\text{out}}$ , driven by the pressure gradient, Darcy's law can be expressed as:

$$\dot{m}_{\text{out}} = -(2\pi r_o) \frac{k k_{\text{rel},g}}{\mu_g} \left( \rho_g \frac{dp_g}{dr} \right)_{r_o} \quad (5)$$

where the pressure gradient is evaluated near the boundary of the control volume.

**Ideal Gas Law in the Control Volume.** The gas flow out of the control volume can also be related to the change in mass of gas  $M_g$  contained in the control volume by the ideal gas law. By taking the derivative of the ideal gas law with respect to time, it is found that:

$$\bar{V}_g \left( \frac{dp_g}{dt} \right) + p_g \left( \frac{d\bar{V}_g}{dt} \right) = M_g R_g \frac{dT}{dt} + R_g T \frac{dM_g}{dt} \quad (6)$$

where  $\bar{V}_g = \phi S_g \bar{V}$  is the part of the control volume  $\bar{V}$  that contains gas, and  $p_g$  and  $T$  are characteristic or lumped averages of the control volume pressure and temperature. The pressure changes much more rapidly than the volume of gas (for cases when large pressures are created), so in this idealized conceptual model, the volume derivative in Eq. (6) will be neglected.

**Conservation of Mass.** The rate at which the mass of gas,  $M_g$ , in the control volume changes is also related to the rate of vapor generation,  $\dot{m}_v$ , and the gas outflow rate,  $\dot{m}_{\text{out}}$ :

$$\frac{dM_g}{dt} = \dot{m}_v - \dot{m}_{out} \quad (7)$$

Equations (6) and (7) are combined to give:

$$\dot{m}_{out} = \dot{m}_v + \frac{M_g}{T} \frac{dT}{dt} - \frac{M_g}{p_g} \frac{dp_g}{dt} \quad (8)$$

**Vapor Generation Rate.** The rate  $\dot{m}_v$  at which vapor is generated inside the control volume is computed by assuming, that the relative humidity remains at 100 percent. Vapor pressure lowering may cause the relative humidity to be somewhat less than 100 percent, but this effect is neglected in the heating regime analysis (although not in the cooling regime analysis). Thus, from the ideal gas law for the vapor, it is found that:

$$\dot{m}_v = \frac{\bar{V}_v}{R_v T} \frac{dp_v}{dt} - \frac{M_v}{T} \frac{dT}{dt} \quad (9)$$

where the v-subscript denotes vapor,  $M_v$  is the mass of vapor in the control volume, and  $\bar{V}_v$  is its partial volume. For 100-percent relative humidity, the vapor pressure is the saturation pressure, so  $p_v$  can be related to other thermodynamic variables by the Clapeyron equation and Eq. (9) can be rewritten in the form:

$$\dot{m}_v = \frac{\bar{V}_v}{R_v T} \left( \frac{\rho_v h_{lg}}{T} \right) \frac{dT}{dt} - \frac{M_v}{T} \frac{dT}{dt} \quad (10)$$

where  $h_{l,g}$  is the change in enthalpy for water, from liquid to gas.

**Mass Flow Rate at Control Volume Boundary.** Equations (8) and (10) are now combined to give an expression for the mass flow rate at the control volume boundary. This expression is:

$$\dot{m}_{\text{out}} = \frac{M_v}{T} \left( \frac{h_{lg}}{R_v T} \right) \frac{dT}{dt} + \left( \frac{M_g - M_v}{T} \right) \frac{dT}{dt} - \frac{M_g}{p_g} \frac{dp_g}{dt} \quad (11)$$

The factor  $M_g - M_v$  is the mass of air  $M_{\text{air}}$  in the control volume. Now  $M_g$ ,  $M_v$ , and  $M_{\text{air}}$  are all of the same order of magnitude, as are the quantities  $(dT/dt)/T$  and  $(dp_g/dt)/p_g$ . Thus, since the quantity  $h_{lg}/R_v T$  has a numerical magnitude of about 20 for water, Eq. (11) can be approximated as:

$$\dot{m}_{\text{out}} \approx \frac{M_v}{T} \left( \frac{h_{lg}}{R_v T} \right) \frac{dT}{dt} \quad (12)$$

This relation simply expresses the conclusion that most of the gas flow out of the control volume is composed of the vapor created by heating the initial mass of liquid in the matrix.

**Characteristic Pressure Gradient.** Equation (12) is substituted into Darcy's law, Eq. (5), to yield an expression for the nonhydrostatic pressure gradient at the control volume boundary:

$$\left( \rho_g \frac{dp_g}{dr} \right)_{r_o} = - \frac{\mu_g M_v}{2 \pi r_o k k_{\text{rel},g} T} \left( \frac{h_{lg}}{R_v T} \right) \frac{dT}{dt} = - \frac{\phi S_v \mu_g \rho_v r_o}{2 k k_{\text{rel},g} T} \left( \frac{h_{lg}}{R_v T} \right) \frac{dT}{dt} \quad (13)$$

where  $S_v$  is vapor saturation, and  $\phi$  is porosity. This expression can be used to define a characteristic pressure gradient in terms of other representative quantities after a characteristic or maximum temperature change is determined from the heating rate.

By making the realistic assumption that the maximum temperature occurs before any substantial fraction of the energy addition rate  $Q$  inside the control volume is conducted to distant parts of the medium, the temperature increase in Eq. (27) can be approximated by an energy balance on the control volume:

$$\frac{dT}{dt} \approx \frac{Q}{\pi r_o^2 \rho_s C_s} \quad (14)$$

It has been assumed, that the temperature distribution is governed primarily by heat conduction (Green et al., 1993) and that the thermal properties of the solid medium are representative of the properties of the solid-liquid-gas mixture. Alternatively,  $dT/dt$  can be expressed in terms of the characteristic temperature change  $\Delta T_o$  and the time duration required to obtain this value, which is roughly the thermal diffusion time scale  $L^2/\alpha_s$ , where  $\alpha_s$  is the thermal diffusivity of the solid. This alternative gives the estimate:

$$\frac{dT}{dt} \approx \frac{\alpha_s \Delta T_o}{L^2} \quad (15)$$

Equations (14) and (15) are order-of-magnitude equivalent and are connected by the temperature increase  $\Delta T_o$ . The expression based on  $Q$  is more convenient to use to establish heating rates for laboratory and numerical investigations when the heating rate of the larger system is known. The expression involving  $\Delta T_o$  is more convenient to use to interpret the results of these investigations. Both forms will be carried along in the subsequent discussions.

With these expressions for  $dT/dt$ , a characteristic pressure gradient can be defined:

$$\frac{\Delta p_{go}}{L} \sim \frac{\phi S_{vo} \mu_{go} \alpha_s Q}{k k_{rel,go} \kappa L T_{avg}} \left( \frac{\rho_{vo}}{\rho_{go}} \right) \left( \frac{h_{lg,o}}{R_v T_{avg}} \right) \approx \frac{\phi S_{vo} \mu_{go} \alpha_s \Delta T_o}{k k_{rel,go} L T_{avg}} \left( \frac{\rho_{vo}}{\rho_{go}} \right) \left( \frac{h_{lg,o}}{R_v T_{avg}} \right) \quad (16)$$

where  $S_{vo}$  is the characteristic vapor saturation, and  $\kappa$  is the thermal conductivity. The first form of  $\Delta p_{go}/L$  is derived from Eq. (14) and the second from Eq. (15).

**Dimensionless Darcy's law and Characteristic Gas Velocity.** With this expression for a characteristic pressure, the full Darcy's law can be rewritten in dimensionless form as:

$$\hat{V}_g = - \left( \frac{\mu_{go}}{\mu_g} \right) \left( \frac{k_{rel,g}}{k_{rel,go}} \right) \left( \hat{\nabla} \hat{p}_g - \frac{(\beta_g/\beta_{go})\theta}{Ad_g} \vec{e}_z \right) \quad (17)$$

The dimensionless group  $Ad_g$ , is called the gas Advection Number. The various ratios of viscosity, relative permeability, and thermal expansion coefficient in Eq. (17) are all of order-of-magnitude unity and so could be neglected. The dimensionless pressure gradient and the dimensionless buoyancy are also of order unity. Consequently, the relative importance of pressure gradients and buoyancy with respect to vapor transport depends solely on the magnitude of the dimensionless number  $Ad_g$ . Physical interpretation of  $Ad_g$  is described below.

The gas velocity in Eq. (17) has been made dimensionless by normalizing to a characteristic velocity equal to:

$$V_{go} \sim \frac{\phi S_{vo} \alpha_s Q}{L \kappa T_{avg}} \left( \frac{\rho_{vo}}{\rho_{go}} \right) \left( \frac{h_{lg,o}}{R_v T_{avg}} \right) \approx \frac{\phi S_{vo} \alpha_s \Delta T_o}{L T_{avg}} \left( \frac{\rho_{vo}}{\rho_{go}} \right) \left( \frac{h_{lg,o}}{R_v T_{avg}} \right) \quad (18)$$

19/37

The first form is based on Eq. (14) and the second on Eq. (15).

### Gas Advection Number, $Ad_g$

The dimensionless Darcy's law, Eq. (17) introduced a new dimensionless number, the gas Advection Number,  $Ad_g$ . It is defined in terms of the relevant parameters by:

$$Ad_g = \frac{\phi S_{vo} \alpha_s \mu_{go} Q}{kk_{rel,go} L \rho_{go} g \beta_{go} \kappa \Delta T_o T_{avg}} \left( \frac{\rho_{vo}}{\rho_{go}} \right) \left( \frac{h_{lg,o}}{R_v T_{avg}} \right) \quad (19)$$

$$\approx \frac{\phi S_{vo} \alpha_s \mu_{go}}{kk_{rel,go} L \rho_{go} g \beta_{go} T_{avg}} \left( \frac{\rho_{vo}}{\rho_{go}} \right) \left( \frac{h_{lg,o}}{R_v T_{avg}} \right)$$

where the two alternative forms result from using either Eqs. (14) or (15) to evaluate the characteristic temperature change. The first form of  $Ad_g$  is a combination of independent and dependent parameters, since  $\Delta T_o$  depends on  $Q$ , and so is not a useful dimensionless group. The second form will therefore be used in the following discussions.

The gas Advection Number is physically the ratio of nonbuoyancy pressure gradient to buoyancy body-force gradient. Thus, a value of  $Ad_g > 1$  implies that the gas flow is controlled by pressure gradients, so the advective component of gas velocity will be much larger than the buoyancy-induced component. Conversely, when  $Ad_g < 1$ , gas flow is controlled by buoyancy. When  $Ad_g \approx 1$ , pressure gradients and buoyancy are comparable in their effects and Eq. (17) is then the same as Eq. (1). It should be noted, however, that for  $Ad_g \leq 1$ , the characteristic gas velocity is quite small.

Some of the important factors that determine the magnitude of  $Ad_g$  are: (i) permeability  $k$ —smaller values (tighter porous media) lead to larger values of  $Ad_g$ , (ii) porosity  $\phi$ —smaller values (media that can contain less gas) lead to smaller values of  $Ad_g$ , and (iii) matrix thermal diffusivity  $\alpha_s$ —larger values (equivalent to a more rapid increase in temperature) lead to larger values of  $Ad_g$ .

As can be seen from the second form given for  $Ad_g$  in Eq. (19), neither the heating rate  $Q$  nor the temperature increase  $\Delta T_o$  directly affects the magnitude of  $Ad_g$  (There is a secondary effect given by the average temperature  $T_{avg}$  and the change in fluid properties with temperature.) This lack of dependency on  $Q$  (or  $\Delta T_o$ ) is the result of the fact that  $Ad_g$  is the ratio of two effects, both of which are proportional to  $Q$  (or  $\Delta T_o$ ). Nonetheless, it is required that  $Q > 0$  since otherwise there are no gas pressures or velocities to consider. It should be noted, also, that both the characteristic pressure, Eq. (16), and characteristic velocity, Eq. (17), increase in proportion to  $Q$  or  $\Delta T_o$ ; hence, the flow and the rate of drying out do depend on  $Q$ .

### Characteristic Gas Pressure Buildup Time Scale

According to the heating phase conceptual model, the time duration over which large pressure gradients will be created in the gas phase is roughly the same as the duration needed to obtain a steady-state temperature; that is, the time scale of this phenomenon is the thermal diffusivity characteristic time:

21/37

$$t_o \sim \frac{L^2}{\alpha_s} \quad (20)$$

This expression for the time scale assumes that the heating duration is at least equal to  $L^2/\alpha_s$ . If it is of shorter duration, the maximum pressures will occur near the end of the heating period. The time scale given by Eq. (20) depends on both the geometric size  $L$  of the heated region and the thermal diffusivity,  $\alpha_s$ , of the heated material. A time scale factor can be derived from Eq. (20).

After the gas pressure obtains its maximum value represented by the characteristic pressure, the pressure will slowly decay. The decay time cannot be predicted by this conceptual model, although, if the heating persists, it will be at least as long as the time  $L^2/\alpha_s$  required for the pressure to increase to its maximum.

## TRANSITIONAL PERIOD

Eventually, the temperature of the heated volume approaches a near steady-state and the gas pressure thereafter begins to decrease. The advective gas flow thus decreases in magnitude, although the gas flow is still away from the heat source. As the pressure continues to decrease, the capillary pressure gradient becomes larger than the gas pressure gradient and liquid water begins to flow back toward the heated region. The net flow of water (vapor away from the heated region, liquid toward the heated region) remains near zero for an extended period of time. When the vapor flow has decreased sufficiently, however, there is a net flow of water back toward the heated region. This point represents the initiation of the cooling period.

A separate conceptual model is not developed specifically for the transitional period. The model developed below for the cooling period is of a general form and could be adapted to the transitional period, if necessary.

## CONCEPTUAL MODEL FOR THE COOLING PERIOD

In the cooling period, the heat generation rate is negligible compared to that during the heating period, and the temperature distribution gradually equalizes throughout the medium. As a result, the water initially driven away from the heat source moves back toward the dried-out region as both liquid and vapor. The primary thermohydrologic concern during this period is the time required to complete this rewetting as a function of the medium geometry, physical properties, and initial heating rate. Just as for the heating period, a conceptual model of the rewetting is desirable to (i) delineate the dominant phenomena, and (ii) ensure that laboratory and field experiments are designed and interpreted correctly with respect to repository behavior. The first part in the development of an idealized conceptual model for the cooling period is to estimate the capillary pressure gradients.

**Pressure Gradients.** For the cooling phase conceptual model, the liquid pressure is expressed as the sum of the gas pressure impressed on the liquid and the pressure difference between the gas and the liquid:

$$p_l = p_g + p_{lg} \quad (21)$$

where the subscript  $l$  denotes liquid. The pressure difference,  $p_{lg}$ , is the negative of the capillary pressure,  $p_c$  (where the negative sign is used so that  $p_{lg}$  itself is a positive value). Further, to ensure that only pressure gradients that create motion are considered,  $p_c$  is written relative to the equilibrium pressure,  $p_{ce}$ , that balances the gravitational gradient. Hence:

$$p_{llg} = -p_c + p_{ce} + (\rho_{lo}gz - p_{ce}) - \rho_{lo}gz \quad (22)$$

The quantity in parentheses in Eq. (22) is equal to zero, and the sum of the first two terms is defined as  $-\Delta p_c$ , which is the nonhydrostatic component of capillary pressure.

The nonhydrostatic capillary pressure is a function of pore size  $d$ , liquid saturation  $S_l$ , and liquid surface tension  $\sigma$  (or some other surface property such as adhesion), and whether the liquid wets the medium. Since water wets the media of interest here, the gradient of nonhydrostatic pressure can be expressed in the general form:

$$\nabla (\Delta p_c) = \frac{\partial \Delta p_c}{\partial S_l} \nabla S_l + \frac{\partial \Delta p_c}{\partial d} \nabla d + \frac{\partial \Delta p_c}{\partial \sigma} \frac{d\sigma}{dT} \nabla T \quad (23)$$

where the gradient of  $\sigma$  has been written in a way to show explicitly its dependence on temperature  $T$ . For the conceptual model, an equivalent continuum model is adopted, so the variation of capillary with respect to  $d$  is neglected. Further, although surface tension gradients may not be totally unimportant during rewetting, they are neglected here for simplicity. Thus, Eq. (23) is expressed here simply as:

$$\nabla (\Delta p_c) = \frac{d\Delta p_c}{dS_l} \nabla S_l \quad (24)$$

Since  $d\Delta p_c/dS_l < 0$ , Eq. (24) demonstrates that  $\Delta p_c$  increases in the direction in which the saturation decreases and roughly in proportion to it.

**Characteristic Darcy's law.** With these definitions and simplifications, Darcy's law for liquid transport is expressed as:

$$\vec{V}_l = -\frac{kk_{rel,l}}{\mu_l} \left( \nabla p_g - \frac{d\Delta p_c}{dS_l} \nabla S_l - \rho_{lo} \mathbf{g} \vec{e}_z + \rho_l \mathbf{g} \vec{e}_z \right) \quad (25)$$

According to the Boussinesq assumption, the net gravitational gradient can be expressed in terms of the temperature change  $\Delta T$  from ambient and the liquid expansion coefficient  $\beta_l$ , with the result that:

$$\vec{V}_l = -\frac{kk_{rel,l}}{\mu_l} \left( \nabla p_g - \frac{d\Delta p_c}{dS_l} \nabla S_l - \rho_{lo} \beta_l \mathbf{g} \Delta T \vec{e}_z \right) \quad (26)$$

For the general model, the capillary pressure  $\Delta p_c$  in Eq. (26) is made dimensionless by dividing it by the characteristic gas pressure of the heating period. This choice for the characteristic gas pressure recognizes the fact, that during the transition period, the gas pressure gradient and the capillary pressure gradient can be comparable in magnitude although opposite in sign. Consequently, the dimensionless Darcy's law for the general case is:

$$\hat{V}_l = -\frac{\mu_{lo} k_{rel,l}}{\mu_l k_{rel,lo}} \left[ \hat{\nabla} \hat{p}_g - \frac{d\Delta \hat{p}_c}{dS_l} \nabla S_l - \frac{(\beta_l/\beta_{lo})\theta}{Ad_l} \mathbf{g} \vec{e}_z \right] \quad (27)$$

and the corresponding characteristic liquid velocity is:

$$V_{lo} = \left( \frac{\mu_{go}}{\mu_{lo}} \right) \left( \frac{k_{rel,lo}}{k_{rel,go}} \right) V_{go} \quad (28)$$

For this case, the dimensionless liquid Advection Number  $Ad_l$  in Eq. (27) is defined as:

$$Ad_l = \left( \frac{\rho_{go}}{\rho_{lo}} \right) \left( \frac{\beta_{go}}{\beta_{lo}} \right) Ad_g \quad (29)$$

When only the cooling period is considered the capillary pressure gradient is no longer coupled to the heating period. Consequently, a more appropriate characteristic pressure for the cooling period is the capillary pressure,  $\Delta p_{co}$ , created by the characteristic decrease in liquid saturation,  $\Delta S_{lo}$ , of the dried-out region. Hence, the appropriate characteristic liquid velocity for the cooling period is:

$$V_{lo} = \left( \frac{k k_{rel,lo}}{\mu_{lo}} \right) \left( \frac{d\Delta p_{co}}{dS_l} \right) \left( \frac{\Delta S_{lo}}{L} \right) \quad (30)$$

Following a similar procedure again in Darcy's law, it is found that the liquid Advection Number for the cooling phase is defined as:

$$Ad_l = \frac{\Delta p_{co} \Delta S_{lo}}{\rho_{lo} \beta_l L g \Delta T_o} \quad (31)$$

The interpretation of  $Ad_l$  is similar to  $Ad_g$ , namely,  $Ad_l > 1$  implies that capillary pressure gradients are much larger than buoyancy gradients.

### Rewetting by Liquid Advection

The characteristic liquid velocity for the cooling phase, as mentioned previously, water can be transported during the cooling phase back to the vicinity of the heat source both as vapor and as liquid. Considering first only the liquid-phase transport, an estimate of the time duration required for the liquid saturation to regain its initial, pre-heated level can be determined by the characteristic liquid velocity given by Eq. (31). Letting the characteristic drop in liquid saturation during the heating region be represented by  $\Delta S_l$ , the mass of liquid  $\Delta M_l$  that must be replaced during rewetting is about  $\bar{V} \phi \rho_{lo} \Delta S_l$ , where  $\bar{V}$  is the affected volume (roughly equivalent to the control volume shown in Figure 1). The rewetting mass

flow rate is roughly  $A \rho_{lo} V_l$ , where  $A$  is the area bounding the volume  $\bar{V}$ . Thus, the time required to rewet the dried-out zone by liquid flow alone is:

$$\begin{aligned}
 t_o &= \left[ \frac{(\mu_{lo}/\mu_{go})(k_{rel,go}/k_{rel,lo})(T_{avg}/\Delta T_o)}{S_{vo}(h_{igo}/R_v T_{avg})(\rho_{vo}/\rho_{go})(\Delta \hat{p}_c/\Delta S_l)} \right] \left( \frac{L^2}{\alpha_s} \right) \\
 &= \frac{\phi \mu_{lo} L^2}{kk_{rel,lo}(d\Delta p_{co}/dS_l)}
 \end{aligned}
 \tag{32}$$

The first form of the definition of the  $t_l$  given in Eq. (32) is derived from the general model (valid for both the transition and the cooling periods). This form demonstrates that the rewetting period is proportional to the time required to obtain the maximum gas pressure during the heating period; it is convenient when experimental values of this time and of the maximum gas pressure are available to evaluate  $L^2/\alpha_s$  and  $\Delta \hat{p}_c$ . The second form of the definition of  $t_l$  in Eq. (32) is derived from the cooling period model; this form is convenient when a moisture release curve or model is available to evaluate  $d\Delta p_{co}/dS_l$  but no other experimental data are available. Note that in both definitions the explicit dependence on the characteristic saturation decrease  $\Delta S_{lo}$  cancels out. However,  $\Delta S_{lo}$  must be estimated to compute appropriate values for  $k_{rel,lo}$  and  $\Delta p_{co}$ . This estimate can, in principle, be obtained from the relations derived for the heating period. However, the estimate is likely to be fairly crude because the heating phase conceptual model is capable of making predictions only to within an order of magnitude, and the total range of  $\Delta S_{lo}$  is typically only one order of magnitude. Thus, a more reasonable approach is to assume that  $\Delta S_{lo}$  is about 0.5, which is the approach taken here.

27/37

**Rewetting Time Similitude.** Equation (32) represents the similarity relation that can be used to interpret or scale-up laboratory and field tests.

### Rewetting by Vapor Diffusion

Diffusion of vapor into the dried-out region followed by condensation can also contribute to rewetting the dried-out region. The diffusion is driven by the vapor partial pressure gradient created by vapor pressure lowering in zones of low liquid saturation. This kind of vapor pressure gradient has also been called a relative humidity gradient.

**Vapor Mass Flux.** For Fickian diffusion, the vapor flux is given by:

$$\bar{q}_v = \tau \phi S_v \rho_v D \nabla w_v \quad (33)$$

where  $\tau$  is tortuosity. The mass fraction  $w_v$  can be determined in terms of the partial pressure  $p_v$  of the vapor as follows:

$$w_v = \frac{M_v}{M_g} = \frac{M_v}{M_v + M_a} = \frac{M_v}{M_v + 1.61 M_v (p_a/p_v)} = \frac{p_v}{p_g + 0.61 p_a} \quad (34)$$

where the ideal gas law has been used, and the numerical factor 1.61 is the ratio of the gas constants for water vapor and air; note that  $p_g = p_a + p_v$ .

During the rewetting period, the total gas pressure  $p_g$  remains approximately constant and equal to ambient throughout the region of interest. Thus, a vapor pressure gradient is accompanied by an approximately equal air partial pressure gradient in the opposite direction. Consequently, the gradient of vapor mass fraction can be found from Eq. (34) to be:

$$\nabla w_v = \left[ \frac{p_g + 1.22p_a}{(p_g + 0.61p_a)^2} \right] \nabla p_v \approx \left( \frac{1}{2p_v} \right) \nabla p_v \quad (35)$$

(The last approximation follows from the assumption that the partial pressures of air and vapor in the mixture are roughly the same).

**Rewetting Times.** The mass flow of vapor into the dried-out region is given by the product of the mass flux and the flow area. The time required for this flow to increase the liquid saturation solely by condensation to its initial saturation level is thus about:

$$t_o = \left( \frac{\rho_{lo}}{\rho_{vo}} \right) \left( \frac{\Delta S_{lo}}{\tau S_v} \right) \left( \frac{p_v}{\Delta p_v} \right) \frac{L^2}{D} \quad (36)$$

where  $\Delta p_v$  is the magnitude of the vapor pressure difference. This relation can be compared to the liquid-flow rewetting time estimate by noting that  $D$  has a value that is approximately 30 times larger than the thermal diffusion coefficient  $\alpha_s$ . Thus:

$$t_g \approx 0.03 \left( \frac{\rho_{lo}}{\rho_{vo}} \right) \left( \frac{\Delta S_l}{\tau S_v} \right) \left( \frac{p_v}{\Delta p_v} \right) \frac{L^2}{\alpha_s} \quad (37)$$

**Rewetting Time Similitude.** Although the contribution of vapor diffusion to rewetting is less important than liquid water flow in most cases, Eqs. (36) and (37) provide a similarity relation to interpret laboratory and field tests for those cases in which vapor mass diffusion should be considered.

## CONCLUSIONS

This study focused on the coupled thermal and hydrological phenomena occurring in a locally-heated, partially saturated porous medium, emphasizing the redistribution of moisture. The motivation of the work is to be able to study selected aspects of the proposed HLW repository at YM using laboratory- or field-scale physical models. Because the general theory of two-phase, two-component flow is too complicated to provide guidance for the design of experiments, several simplified analytical conceptual models were developed. Different conceptual models were formulated specifically to determine (i) when moisture redistribution by gas phase transport during heating would be driven predominantly by pressure gradients as opposed to buoyancy, and (ii) after heating ceases, the time required to re-wet the dried out volume near the heat sources by either liquid or vapor transport. The models were predicted on a thermal evolution model for the repository that can be divided into three periods: (i) heating, (ii) transitional, and (iii) cooling. The models were characterized in terms of dimensionless parameters and used to establish scaling laws that relate heat and mass transfer mechanisms at the laboratory ( $10^{-1}$  to  $10^0$  m), field ( $10^1$  m) and mountain ( $10^2$  to  $10^3$  m) scales.

**Heating Period Model.** The conceptual model of the heating period demonstrated that the requirements for similarity among systems of various geometric sizes and thermohydrologic properties are summarized in a new dimensionless number called the gas Advection Number,  $Ad_g$ . Like other dimensionless numbers,  $Ad_g$  is the ratio of two physical effects, in this case the ratio of gas pressure gradients created by the confining effect of the medium to buoyancy-induced body forces.  $Ad_g$  is formally expressed in terms of thermohydrologic parameters such as permeability and porosity, fluid parameters such as density, viscosity,

and coefficient of thermal expansion, and heating rate parameters such as the temperature increase of the media near the heater.

For cases where  $Ad_g > 1$ , the heating is sufficient to cause the creation of large pressure gradients and high advective gas flows. Under these conditions, the region near the heat source is likely to experience a significant degree of drying. The model also predicts the magnitude of the peak gas pressure gradient that will be produced. The time at which the peak gas pressure occurs is predicted to be the same as the characteristic thermal diffusion time. For cases where  $Ad_g \leq 1$ , heating is expected to produce only small gas flows away from the heat source and buoyancy has a dominant role in setting the characteristics of fluid flow. For these conditions, less drying of the repository is expected.

**Cooling Period Model.** The most important aspect of moisture redistribution during the cooling period is the time required to rewet the region dried out during the heating period. Rewetting time is important because it is a measure of when water comes back into contact with the canister environment after it has been dried out. This rewetting aspect was investigated using the cooling period conceptual model. Analogous to the heating period, a liquid Advection Number  $Ad_l$  was developed. The rewetting response of various systems is expected to be similar when the values of  $Ad_l E$  are of a similar order of magnitude for the systems.

The cooling period conceptual model considered rewetting both by liquid transport and by vapor phase diffusion. Liquid transport rewetting flow occurs primarily in the matrix even for fractured media, because of the large capillary pressure gradients created in the matrix by the drying during the heating phase.

Hence, the conceptual model of the cooling period should apply equally to fractured or nonfractured media. In all cases studied, the model predicted that rewetting due to vapor diffusion was negligibly small.

**Scaling Implications of the Conceptual Model.** The conceptual models were developed to evaluate laboratory- and field-scale experiments as analogues of repository responses to heating. The pressure, velocity, and time scaling laws that arise in the conceptual model can also be used to interpret, or scale-up, the responses measured in laboratory- and field-scale experiments in terms of repository responses, when the thermohydrologic and heating rate conditions of the experiments are considered to be sufficiently similar. Likewise, the models can be used to guide numerical simulations of these responses. In addition, the dimensionless terms developed as part of the scaling laws are useful in the identification of different classes of flow regimes formed as a function a specific heat load.

## VARIABLES

$Ad_g$  = gas advection number (-)

$Ad_l$  = liquid advection number (-)

$C_s$  = specific heat of solid (J/kg-K)

$d$  = pore size (m)

$D$  = binary gas diffusion coefficient (m<sup>2</sup>/s)

$\vec{e}_z$  = unit vector in z direction

- $g$  = acceleration of gravity (m/s)
- $h$  = fluid enthalpy per unit mass (J/kg)
- $h_{lg}$  = change in enthalpy for water, from liquid to gas ( $h_{lg} = 2,400$  kJ/kg at approximately 40 °C)
- $k$  = permeability ( $m^2$ )
- $k_{rel,i}$  = relative permeability (-)
- $L$  = characteristic length scale (-)
- $\dot{m}_{out}$  = gas flow out of the control volume ( $kg/m^3-s$ )
- $\dot{m}_{evap}$  = rate at which liquid water is evaporated per unit volume, negative if vapor is condensed  
( $kg/m^3-s$ )
- $\dot{m}_v$  = rate of vapor generation of the control volume ( $kg/m^3-s$ )
- $M$  = mass contained in the control volume (kg)
- $p$  = fluid pressure (Pa)
- $p_c$  = suction (capillary pressure) (Pa)
- $p_v$  = partial pressure of the vapor (Pa)
- $p_{sat}$  = thermodynamic saturation pressure of the pure substance (Pa)
- $p_{lg}$  = pressure difference between gas and liquid (Pa)
- $p_e$  = Peclet number,  $V_g L/D$ , (-)
- $\bar{q}_i$  = mass flux of the  $i^{th}$  component ( $kg/m^2-s$ )

- $\bar{q}_v$  = mass diffusion flux of the vapor through the gas mixture ( $\text{kg/m}^2\text{-s}$ )  
 $Q$  = heat sink/source rate of energy addition per unit volume ( $\text{W/m}^3$ )  
 $r_o$  = reference radius of control volume (m)  
 $R_v$  = ideal gas constant for the pure substance ( $\text{J/kg-K}$ )  
 $S$  = saturation (-)  
 $S_g$  = saturation level of gas (-)  
 $S_{v_o}$  = characteristic vapor saturation (-)  
 $t$  = time (s)  
 $T$  = temperature (K)  
 $\Delta T_o$  = temperature change from the reference condition (K)  
 $u$  = fluid internal energy per unit mass ( $\text{J/kg}$ )  
 $\vec{V}$  = fluid velocity (m/s)  
 $\vec{V}_g$  = Darcy velocity (advection) of the gas (m/s)  
 $\bar{V}$  = control volume ( $\text{m}^3$ )  
 $w_a$  = mass fraction of air in the gas mixture (-)  
 $w_v$  = mass fraction of water vapor in the gas mixture (-)  
 $\alpha_s$  = bulk thermal diffusivity of saturated medium ( $\text{m}^2/\text{s}$ )

- $\beta_i$  = thermal expansion coefficient of the  $i^{\text{th}}$  component ( $\text{K}^{-1}$ )  
 $\kappa$  = thermal conductivity of the gas-liquid-solid combination ( $\text{w/m-k}$ )  
 $\rho$  = fluid density ( $\text{kg/m}^3$ )  
 $\rho_g$  = density of gas ( $\text{kg/m}^3$ )  
 $\phi$  = porosity (-)  
 $\rho_w$  = reference density ( $\text{kg/m}^3$ )  
 $\rho_s$  = density of the solid  
 $\sigma$  = surface tension ( $\text{n/m}$ )  
 $\tau$  = tortuosity (-)  
 $\theta$  =  $\Delta T / \Delta T_o$ , nondimensional temperature change (-)  
 $\mu$  = fluid viscosity ( $\text{Pa-s}$ )  
 $\nu$  = kinematic viscosity ( $\text{m}^2/\text{s}$ )

#### ACKNOWLEDGEMENT

This paper was prepared to document work performed by the Center for Nuclear Waste Regulatory Analyses (CNWRA) for the U.S. Nuclear Regulatory Commission (NRC) under Contract No. NRC-02-93-005. The activities reported here were performed on behalf of the NRC Office of Nuclear Material Safety

and Safeguards (NMSS), Division of Waste Management (DWM). This paper is an independent product of the CNWRA and does not necessarily reflect the views or regulatory position of the NRC.

## REFERENCES

- Andrews, R.W., T.F. Dale, and J.A. McNeish. 1994. *Total System Performance Assessment-1993: An Evaluation of the Potential Yucca Mountain Repository*. Las Vegas, NV: INTERA, Inc.
- Baker, W.E., P.S. Westine, and F.T. Dodge. 1973. *Similarity Methods in Engineering Dynamics*. Rochelle Park, NJ: Hayden Book Co.
- Bear, J. 1972. *Dynamics of Fluids in Porous Media*. New York, NY: Dover Publications.
- Buscheck, T.A., and J.J. Nitao. 1992. The impact of thermal loading on repository performance at Yucca Mountain. *Proceedings of the Third Annual International Conference on High-Level Radioactive Waste Management*. La Grange Park, IL: American Nuclear Society: 1,003–1,017.
- Buscheck, T.A., and J.J. Nitao. 1993. The analysis of repository-heat-driven hydrothermal flow at Yucca Mountain. *Proceedings of the Fourth Annual International High-Level Radioactive Waste Management Conference*. La Grange Park, IL: American Nuclear Society: 846–867.
- Buscheck, T.A., and J.J. Nitao. 1994. The impact of buoyant, gas-phase flow and heterogeneity on thermo-hydrological behavior at Yucca Mountain. *Proceedings of the Fifth Annual International High-Level Radioactive Waste Management Conference*. La Grange Park, IL: American Nuclear Society: 27–74.
- Corey, A.T. 1986. *Mechanics of Immiscible Fluids in Porous Media*. Littleton, CO: Water Resources Publications.

36/31

- Fox, R.W., and A.T. McDonald. 1978. *Introduction to Fluid Mechanics*. New York, NY: McGraw-Hill Publishing Co.
- Green, R.T., R.D. Manteufel, F.T. Dodge, and S.J. Svedeman. 1993. *Theoretical and Experimental Investigation of Thermohydrologic Processes in a Partially Saturated, Fractured Porous Medium*. NUREG/CR-6026. Washington, DC: Nuclear Regulatory Commission.
- Green, R.T., F.T. Dodge, S.J. Svedeman, R.D. Manteufel, G. Rice, K.A. Meyer, and R.G. Baca. 1995. *Thermally Driven Moisture Redistribution in Partially Saturated Porous Media*. NUREG/CR-6348. Washington, DC: Nuclear Regulatory Commission
- Lichtner, P.C., and J. Walton. 1994. *Near-Field Liquid-Vapor Transport in a Partially Saturated High-Level Nuclear Waste Repository*. CNWRA 94-022. San Antonio, TX: Center for Nuclear Waste Regulatory Analyses.
- Miller, E.E. 1980. Similitude and scaling of soil-water phenomena. *Applications of Soil Physics*. D. Hillel, ed. New York, NY: Academic Press: 300–318.
- Narasimhan, T.N. 1982. Physics of saturated-unsaturated subsurface flow. *Geological Society of America*. Special Paper 189.
- Nitao, J.J., T.A. Buscheck, and D.A. Chesnut. 1992. The implication of episodic nonequilibrium fracture-matrix flow on site suitability and total system performance. *Proceedings, of the Third High Level Radioactive Waste Management International Conference*: Las Vegas, NV.
- Pruess, K. 1985. *A Quantitative Model of Vapor Dominated Geothermal Reservoirs as Heat Pipes in Fractured Porous Rock*. LBL-19366. Berkeley, CA: Lawrence Berkeley Laboratory.

- Pruess, K., and Y. Tsang. 1993. Modeling of strongly heat-driven flow processes at a potential high-level nuclear waste repository at Yucca Mountain, Nevada. *Proceedings at the Fourth Annual International Conference on High-Level Radioactive Waste Management*. Las Vegas, NV.
- Pruess, K., and Y. Tsang. 1994. Thermal modeling for a potential high-level nuclear waste repository at Yucca Mountain, Nevada. LBL-35381. *Lawrence Berkeley Laboratory Report*.
- Ramirez, A.L., ed. 1991. *Prototype Engineered Barrier System Field Test (PEBSFT) Final Report*. UCRL-ID-106159. Livermore, CA: Lawrence Livermore National Laboratory.
- Ramspott, L.D. 1991. The constructive use of heat in an unsaturated tuff repository. *Proceedings of the Second Annual High-Level Radioactive Waste Management Conference*. La Grange Park, IL: American Nuclear Society: 1,602–1,607.
- Rasmussen, T.C., and D.D. Evans. 1989. *Fluid Flow and Solute Transport Modeling Through Three-Dimensional Networks of Variably Saturated Discrete Fractures*. NUREG/CR-5239. Washington, DC: Nuclear Regulatory Commission.
- Wang, J.S.Y., and T.N. Narasimhan. 1986. *Hydrologic Mechanisms Governing Partially Saturated Fluid Flow in Fractured Welded Units and Porous Nonwelded Units at Yucca Mountain*. LBL-21022. Berkeley, CA: Lawrence Berkeley Laboratory.
- Wilder, D.G. 1993. Alternative strategies—a means for saving money and time on the Yucca Mountain project. *Proceedings of the Fourth High-Level Radioactive Waste Management International Conference*: Las Vegas, NV.
- Zimmerman, R.M., M.L. Blanford, J.F. Holland, R.L. Schuch, W.H. Barrett. 1986. *Final Report G-Tunnel Small-Diameter Heater Experiments*. SAND84-2621. Albuquerque, NM: Sandia National Laboratories.